Dynamical Casimir Effect in Quantum Information Processing

Giuliano Benenti,[1,2] Antonio D'Arrigo,[3,4] Stefano Siccardi,[5] and Giuliano Strini[5]

[1] *CNISM and Center for Nonlinear and Complex Systems, Università degli Studi dell'Insubria, via Valleggio 11, 22100 Como, Italy*
[2] *Istituto Nazionale di Fisica Nucleare, Sezione di Milano, via Celoria 16, 20133 Milano, Italy*
[3] *CNR-IMM UOS Università (MATIS), Consiglio Nazionale delle Ricerche, Via Santa Sofia 64, 95123 Catania, Italy*
[4] *Dipartimento di Fisica e Astronomia, Università degli Studi Catania, Via Santa Sofia 64, 95123 Catania, Italy*
[5] *Department of Physics, University of Milan, via Celoria 16, 20133 Milano, Italy*

We demonstrate, in the regime of ultrastrong matter-field coupling, the strong connection between the dynamical Casimir effect (DCE) and the performance of quantum information protocols. Our results are illustrated by means of a realistic quantum communication channel and show that the DCE is a fundamental limit for quantum computation and communication and that novel schemes are required to implement ultrafast and reliable quantum gates. Strategies to partially counteract the DCE are also discussed.

PACS numbers: 42.50.Ct, 03.67.Hk, 03.67.-a

arXiv:1407.7567v1 [quant-ph] 28 Jul 2014

Introduction. The search for high-speed operations is vital in quantum information [2, 6]. The clock time of a quantum computer, that is the time for the execution of a quantum gate, should be much shorter than the decoherence time scale to allow fault-tolerant quantum computation. Moreover, the enhancement of transmission rates in quantum channels is crucial to widen the applicability domain of quantum cryptography and quantum networks. The possibility of speeding up quantum operations is nowadays offered by circuit quantum electrodynamics (QED) [3, 4], where one can address the ultrastrong coupling regime of light-matter interaction. In this regime, the coupling strength g becomes comparable to the resonator frequency ω [5–7].

The dynamical Casimir effect (DCE) [8, 9], that is, the generation of photons from the vacuum due to time-dependent boundary conditions, has deep connections [10] with other quantum vacuum amplification mechanisms such as the the Hawking radiation released by black holes [11] and the Unruh effect for an accelerated observer [12]. Recently, the DCE has been demonstrated experimentally in superconducting circuit QED [13, 14]. Since a rapid variation of the matter-field coupling is needed to implement ultrafast quantum gates, the DCE appears as a fundamental limit to the realization of high-speed quantum information protocols. In this context, it is useful to remark that the coupling strength $g \propto 1/\sqrt{V}$, with V the quantization volume for the field, so that the DCE can be equally generated by a time-dependent coupling constant rather than by time-dependent boundary conditions [9, 15, 16].

In this paper, we demonstrate the strong impact of photon emission by the DCE on quantum information processing. We consider a quantum channel for the coherent transfer of any unknown quantum state from qubit 1 (Q_1) to qubit 2 (Q_2), mediated by a single mode of the quantized electromagnetic field (cavity mode C). This is a genuine prototype of a *quantum-bus*, which allows to reliably move quantum information and share entanglement between different units of a quantum computing architecture. The transmission capability of such communication channel is quantified by its *quantum capacity* [17, 18], and therefore by the channel coherent information [19], which critically depends on the coupling strength g. While the system allows for a perfect transmission in the rotating-wave approximation (RWA) (i.e., in the limit $g/\omega \ll 1$), in the ultrastrong coupling regime terms beyond the RWA lead to the generation of photons [20, 21], thus spoiling the channel ability to convey quantum information, up to prevent any reliable communication for very high g. On the other hand, strong coupling is needed for fast transmission. Therefore we use the quantum information transmission rate (number of reliably transmitted qubits per unit time) as a figure of merit for the channel performance. It is remarkable that the transmission rate is optimized for values of g belonging to the ultrastrong coupling regime. As a proof of the strong connection between the DCE and channel performance, we show that the mean number of emitted photons is anticorrelated with the coherent information transmitted down the channel. Finally, we discuss strategies suitable to partially counteract photon generation by the DCE. We should stress that the quantum channel discussed in this paper follows steps already experimentally implemented by superconducting qubits coupled through a resonant cavity [22].

Physical model. The qubits-cavity dynamics is described by the Rabi Hamiltonian [23], with switcheable couplings:

$$H(t) = H_0 + H_I(t),$$

$$H_0 = -\frac{1}{2}\sum_{k=1}^{2}\omega_k\sigma_z^{(k)} + \omega\left(a^\dagger a + \frac{1}{2}\right),$$

$$H_I(t) = \sum_{k=1}^{2} f_k(t)\,[\,g_k\,\sigma_+^{(k)}\,(a^\dagger + a), + g_k^\star\sigma_-^{(k)}\,(a^\dagger + a)\,], \tag{1}$$

where we set $\hbar = 1$, $\sigma_i^{(k)}$ $(i = x, y, z)$ are the Pauli matrices for qubit Q_k $(k = 1, 2)$, $\sigma_\pm^{(k)} = \frac{1}{2}\,(\sigma_x^{(k)} \mp i\sigma_y^{(k)})$ are the rising and lowering operators for the two-level system: $\sigma_+^{(k)}|g\rangle_k = |e\rangle_k$, $\sigma_+^{(k)}|e\rangle_k = 0$, $\sigma_-^{(k)}|g\rangle_k = 0$, $\sigma_-^{(k)}|e\rangle_k = |g\rangle_k$; the operators $a^\dagger$ and a create and annihilate a photon: $a^\dagger|n\rangle = \sqrt{n+1}|n+1\rangle$, $a|n\rangle = \sqrt{n}|n-1\rangle$, $|n\rangle$ being the Fock state with n photons. The switching on/off of the couplings is governed by the functions $f_k(t)$, in the manner detailed below. For simplicity's sake, we consider the resonant case ($\omega_1 = \omega_2 \equiv \omega$) and the coupling strengths $g_1 = g_2 \equiv g \in \mathbb{R}$. The RWA is obtained when we neglect the terms $\sigma_+^{(k)}a^\dagger$, which simultaneously excites Q_k and creates a photon, and $\sigma_-^{(k)}a$, which de-excites Q_k and annihilates a photon. In this limit, Hamiltonian (1) reduces to the Jaynes-Cummings Hamiltonian [23], with a switchable coupling. We set $\omega = 1$, so that in the RWA the interaction time needed to transfer an excitation from one qubit to the field or vice versa ($|e\rangle_k|0\rangle \leftrightarrow |g\rangle_k|1\rangle$) is $\tau = \pi/2g$ and the vacuum Rabi frequency $\Omega_0 = g$. We work in the interaction picture, where the effective Hamiltonian at resonance is given by $\tilde{H}(t) = e^{iH_0t}H_I(t)e^{-iH_0t}$ (we will omit the tilde from now on).

Basic quantum protocol. In order to transmit quantum information through the above physical system, we consider the communication protocol $\mathcal{P}_0$ (sketched in Fig. 1), consisting of the following steps:

1. Q_1 is prepared in an arbitrary input state ρ, while Q_2 and the cavity mode C are in their ground state;
2. Q_1 interacts with C, for a time $T_1 = \tau$;
3. the coupling of Q_1 with C is switched off, and both qubits remain non-interacting for a time T_c;
4. Q_2 interacts with C, for a time $T_2 = \tau$;
5. the coupling of Q_2 with C is switched off.

The final state of Q_2 is given by

$$\rho' = \mathrm{Tr}_{\mathsf{Q}_1\mathsf{C}}[U(\rho\otimes|0\rangle\langle 0|\otimes|g\rangle_{22}\langle g|)U^\dagger], \tag{2}$$

with U unitary time evolution operator for $\mathsf{Q}_1\mathsf{C}\mathsf{Q}_2$, determined by the above described quantum protocol. We start by considering sudden switch on/off of the couplings, i.e. $f_1(t) = 1$ for $0 \le t \le T_1$, $f_1(t) = 0$ otherwise; $f_2(t) = 1$ for $T_1 + T_c \le t \le T_1 + T_c + T_2$, $f_2(t) = 0$ otherwise. Moreover, we set $T_c = 0$.

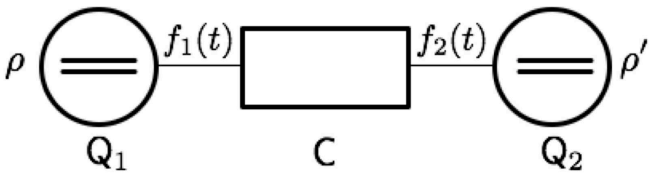

FIG. 1. Schematic drawing of the quantum protocol discussed in the text. The coupling between the qubit Q_i and the cavity C is modulated by the function $f_i(t)$. By initially preparing Q_1 in the state ρ, Q_2 is found in the state ρ' at the end of the protocol.

The quantum channel $\mathcal{E}$, mapping the input state ρ into the output state $\rho' = \mathcal{E}(\rho)$, allows for ideal quantum information transmission, in the RWA regime and for the above suitably chosen values of T_1, T_2, and T_c. Always in this regime, it reduces to the amplitude damping channel for generic T_1, T_2, and T_c. However, when the terms beyond the RWA are taken into account, $\mathcal{E}$ has a non-trivial structure, described in the supplementary material, and the channel performance deteriorates. The computation of the quantum capacity of channel $\mathcal{E}$, defined as the maximum number of qubits that can be reliably transmitted per channel use, is a formidable task, because one should perform an optimization over all possible N-qubit input states, for N uses of the channel and in the limit $N \to \infty$. Hereafter, we limit ourselves to the channel optimization over all possible single-qubit ($N = 1$) input states:

$$Q_1 = \max\left\{\max_\rho\left[I_c(\mathcal{E},\rho)\right], 0\right\},$$
$$I_c(\mathcal{E},\rho) \;=\; S[\mathcal{E}(\rho)] - S_e(\mathcal{E},\rho). \tag{3}$$

Here the quantity I_c is the *coherent information* [19], $S(\rho) = -\mathrm{Tr}[\rho\log_2\rho]$ the von Neumann entropy, and $S_e(\mathcal{E},\rho)$ the *entropy exchange* [24], defined as $S_e(\mathcal{E},\rho) = S[(\mathcal{I}\otimes\mathcal{E})(|\psi\rangle\langle\psi|)]$, where $|\psi\rangle\langle\psi|$ is any purification of ρ. That is, we consider Q_1, described by the density matrix ρ, as a part of a larger quantum system $\mathsf{R}\mathsf{Q}_1$; $\rho = \mathrm{Tr}_{\mathsf{R}}|\psi\rangle\langle\psi|$ and the reference system R evolves trivially, according to the identity superoperator $\mathcal{I}$. Note that, when the optimized coherent information is negative, the single-shot quantum capacity Q_1 vanishes. In the RWA limit $g \to 0$, the ideal transmission (quantum capacity $Q = Q_1 = 1$) is obtained for the fully unpolarized input state $\rho = \rho_u = I/2$. We found numerically that, even in the ultrastrong coupling regime, the optimization over ρ could improve Q_1 only by a tiny amount of the order of 10^{-3} or smaller, with respect to $\rho = \rho_u$. The very good agreement between $I_c(\rho_u)$ (full curve) and Q_1 (gray circles) is shown in Fig. 2. On this basis, in what

follows we will limit ourselves to present data for I_c at $\rho = \rho_u$.

Results. The coherent information I_c as a function of the coupling strength g is shown in Fig. 2 (full curve). This quantity takes the value $I_c = 1$, corresponding to a clean quantum channel, in the RWA limit $g \to 0$. In the ultrastrong coupling regime ($g \gtrsim 0.1$), I_c drops significantly and, for $g \gtrsim 0.42$, becomes negative, so that *the quantum channel can no longer be used to transmit quantum information.* Note that the coherent information is a non-monotonic function of the coupling strength, with maxima at $g_k^{(M)} = 1/(2k\omega + 1)$ and minima at $g_k^{(m)} = 1/(2k\omega)$ ($k = 1, 2, ...$; $\omega = 1$ in our units). This regular structure, with periodicity 2ω for g^{-1}, is a consequence of the terms beyond the RWA in Hamiltonian (1). Indeed, the Bloch vector (of Q_1 when Q_1 and C are coupled or of Q_2 when the interaction is between Q_2 and C) rotates with a speed oscillating with frequency 2ω and therefore also the distance between the exact and the RWA evolution exhibits oscillations of frequency 2ω [25]. The 2ω factor can be clearly seen by expanding, in the interaction picture, the qubit-field state at time t as $|\Psi(t)\rangle = \sum_{l=g,e} \sum_{n=0}^{\infty} C_{l,n} |l, n\rangle$. The time-evolution of the coefficients $C_{l,n}$ is governed by the equations

$$\begin{cases} i\,\dot{C}_{g,n}(t) = \Omega_n\, C_{e,n-1}(t) + \Omega_{n+1} e^{-2i\omega t}\, C_{e,n+1}(t), \\ i\,\dot{C}_{e,n-1}(t) = \Omega_n\, C_{g,n}(t) + \Omega_{n-1} e^{2i\omega t}\, C_{e,n-2}(t), \end{cases} \tag{4}$$

with the Rabi frequencies $\Omega_n = g\sqrt{n}$, where $n = 0, 1, 2, ...$ (the terms $C_{l,m}$ and $\dot{C}_{l,m}$ must be set to zero when $m < 0$). It is interesting to remark that a decay with oscillations in the ultrastrong coupling regime was observed for the fidelity of a quantum gate in Ref. [26].

The strong connection between the channel performance and the DCE is evident from the fact that the coherent information shows a striking anticorrelation of peaks and valleys with the mean number $\langle n \rangle$ of photons in the cavity, both at the end of the protocol (dashed curve in Fig. 2) and for the pure DCE [27] (dotted curve in the same figure). In the latter case, qubit Q_1 and the cavity C are prepared in their ground state ($\rho = \rho_g = |g\rangle_{11}\langle g|$) and the evolution of system $\mathsf{Q}_1\mathsf{C}$ is followed up to time T_1. Note that the evolution of any generic input state $\rho = p|g\rangle_{11}\langle g| + (1-p)|e\rangle_{11}\langle e| + r|g\rangle_{11}\langle e| + r^\star|e\rangle_{11}\langle g|$ also includes the evolution of ρ_g, namely the pure DCE. The photons generated by the pure DCE lead to further, stimulated emission of photons.

Strategies to contrast the DCE. It is clear that suitable strategies must be developed to contrast the DCE in the ultrastrong coupling regime, still allowing ultrafast quantum gates. Here we discuss of two variants of the protocol $\mathcal{P}_0$, in which we act on the switchable couplings $f_i(t)$.

A first possibility (protocol $\mathcal{P}_1$) is to switch on/off the interaction in a less abrupt way, for instance by substituting the rectangular windows for f_1 and f_2 with the

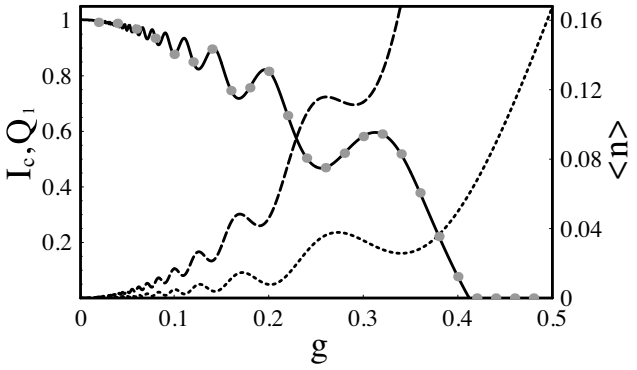

FIG. 2. Coherent information $I_c(\rho_u)$ (full curve, left axis), single-shot quantum capacity Q_1 (gray circles,left axis) and mean photon number $\langle n \rangle$ (right axis) as a function of the qubit-field coupling strength g. The mean photon number is shown for the pure DCE (dotted curve) and at the end of the quantum communication protocol (dashed curve). The time intervals of the protocol are $T_1 = T_2 = \pi/2g$ and $T_c = 0$. As we point out in the text, with a very good approximation $Q_1 \simeq I_c(\rho_u)$. Here and in the following figures the coherent information in computed for the maximally mixed input state ρ_u.

Hamming window

$$f_k(t) = \begin{cases} 1 - \xi \cos(2\pi t_k/T_k) \;\text{ if }\; 0 \le t_k \le T_k, \\ 0 \;\text{ otherwise,} \end{cases} \tag{5}$$

with t_k time from the beginning of the window ($t_1 = t$ and $t_2 = t - (T_1 + T_c)$) and $0 \le \xi \le 1$ ($\xi = 0$ corresponds to the rectangular windows, $\xi = 1$ to continuous functions f_k). The area below the Hamming window is the same as for the rectangular window, since the reduction of coupling strength at the sides of the window is compensated by an increase in its middle. Such window does not affect the RWA perfect transmission, while relevant differences with respect to the rectangular window occur in the ultrastrong coupling regime. We can see from Fig. 3 that the Hamming window leads to a significant improvement of the coherent information in the region $0.1 \lesssim g \lesssim 0.3$, while it can also deteriorate the performance of the channel at larger values of g. Moreover, the oscillations of the rectangular window instance are smoothed. Similar considerations can be applied to the transmission rate R (see the inset of Fig. 3), defined as the ratio between the coherent information and the duration ($T = T_1 + T_c + T_2 = \pi/g$) of the whole quantum protocol. Note that, while the coherent information is maximum in the RWA regime, the transmission rate is maximum at $g \approx 0.3$. This individuate an *optimal coupling value* in the ultrastrong coupling regime, which allows for the most efficient use of the physical resource $\mathsf{Q}_1\mathsf{C}\mathsf{Q}_2$.

As a second strategy (protocol $\mathcal{P}_2$), we optimize over the timing, i.e. we optimize $I_c(\mathcal{E}, \rho_u)$ over T_1, T_2, and T_c. The results of our numerical optimization, with the max-

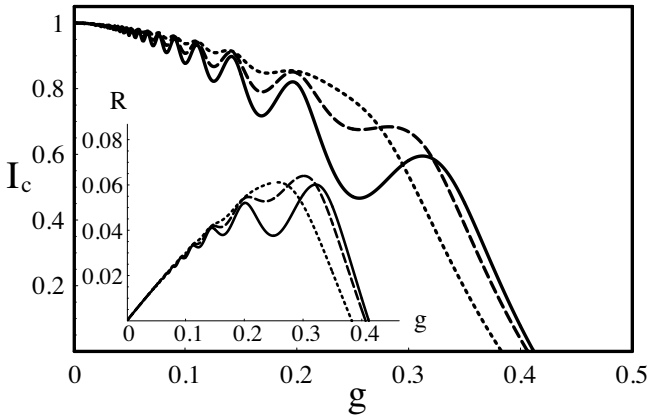

FIG. 3. Coherent information $I_c(\rho_u)$ (main figure) and transmission rate R (inset) as a function of the coupling strength g, for the transmission window discussed in the text, with $\xi = 0$ (full curve), $\xi = 0.2$ (dashed curve), and $\xi = 0.5$ (dotted curve). As in Fig. 2, $T_1 = T_2 = \pi/2g$ and $T_c = 0$.

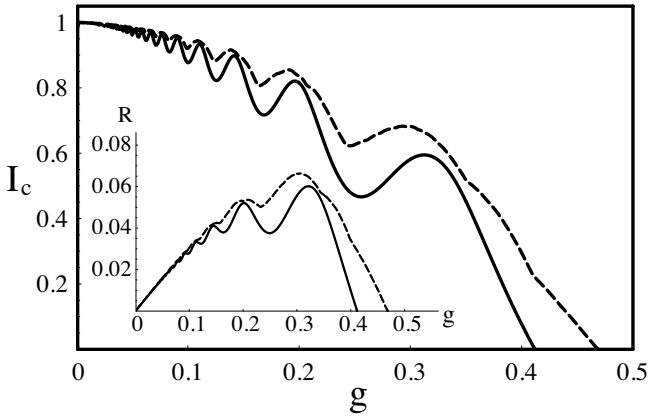

FIG. 4. Coherent information $I_c(\rho_u)$ (main figure) and transmission rate R (inset) as a function of the coupling strength g, for the standard protocol (full curve) and after optimization over the times T_1, T_2, and T_c.

ima of I_c searched in the intervals $T_1, T_2 \in [0.8, 1.2]$ and $T_c \in [0, 2\pi]$, are shown in Fig. 4 (dashed curve). We can appreciate a significant enhancement of I_c with respect to the standard timing discussed above (full curve). Moreover, quantum information transmission becomes possible up to $g \approx 0.47$. Similar results are obtained also for the optimized transmission rate, see the inset of Fig. 4. It is worth noting that also for protocol $\mathcal{P}_2$ the optimality of the coupling near $g = 0.3$ is confirmed.

Discussion. Our analysis deals with the dynamical Casimir effect (DCE) in the field of quantum information processing, paving the way to further investigations. In this paper we address the aptitude to convey quantum information between two qubits Q_1 and Q_2, through a cavity C. The emergence of the DCE in the ultrastrong coupling regime seems to put an intrinsic limit to the capability of the bus $\mathsf{Q}_1\mathsf{C}\mathsf{Q}_2$ to transmit quantum information: when $g \gtrsim 0.5$ it happens that $Q_1 = 0$. Several open questions remain. We have no evidence that the coherent information of the channel $\mathsf{Q}_1\mathsf{C}\mathsf{Q}_2$ is subadditive, therefore one can wonder if entanglement in the input state over different channel uses can counteract the deleterious effect of the DCE. Moreover, after a channel use, the cavity remains populated, as it shown in Fig. 2 (dashed curve). Some time has to be elapsed in order to reset the cavity to its ground state, for instance by a suitable local control. If instead, in order to increase the transmission rate, the cavity mode is not reset after each channel use [28, 29], one should consider a quantum channel with memory effects [30]. Can memory effects be useful in order to improve the channel performance?

While we have investigated two variants, $\mathcal{P}_1$ and $\mathcal{P}_2$ of the basic protocol $\mathcal{P}_0$, other improvements are surely possible, for instance taking into account separately the various steps of $\mathcal{P}_0$. The transmission of quantum information is realized by two consecutive channels, $\mathcal{E} = \mathcal{E}_2 \circ \mathcal{E}_1$, where $\mathcal{E}_1 : \mathsf{Q}_1 \to \mathsf{C}$ and $\mathcal{E}_2 : \mathsf{C} \to \mathsf{Q}_2$. By a numerical analysis we found that the channel $\mathcal{E}_1$ succeeds in reliably transmitting quantum information from the first qubit to the cavity, also in cases when $Q_1 = 0$; for example for $g = 0.5$ we have that $Q^{(\mathcal{E}_1)} > 0.75$. It is the further processing of the quantum information by $\mathcal{E}_2$ which produces a vanishing Q_1. After the first channel, the information is spread up over different levels of the cavity as a consequence of the DCE: this is the cause that prevents the second channel to work properly. Modification of the basic protocol $\mathcal{P}_0$ and novel schemes could be studied in order to contrast the DCE, taking into account the different performances of quantum channels $\mathcal{E}_1$ and $\mathcal{E}_2$. Techniques such as the quantum optimal control [31] might be useful, or one could also take inspiration from counterintuitive protocols for population transfer in stimulated Raman adiabatic passage (STIRAP) [32].

To summarize, we have illustrated in the regime of ultrastrong matter-field coupling the connection between the dynamical Casimir effect and the performance of quantum information protocols. Since the ultrastrong regime is already investigated in circuit QED experiments, it can be foreseen that the DCE will play for quantum computation and communication a role similar to the one played by the (static) Casimir effect in the development of nanomechanical tecnologies [33].

G.B. acknowledges the support by MIUR-PRIN project "Collective quantum phenomena: From strongly correlated systems to quantum simulators". A.D. acknowledges support from CSFNSM Catania.

[1] G. Benenti, G. Casati, and G. Strini, *Principles of Quantum Computation and Information*, Vol. I: Basic concepts (World Scientific, Singapore, 2004); Vol. II: Basic tools

and special topics (World Scientific, Singapore, 2007).
[2] M. A. Nielsen and I. L. Chuang, *Quantum computation and quantum information* (Cambridge University Press, Cambridge, 2000).
[3] A. Blais, R.-S. Huang, A. Wallraff, S. M. Girvin, and R. J. Schoelkopf, Phys. Rev. A **69**, 062320 (2004).
[4] A. Wallraff, D. I. Schuster, A. Blais, L. Frunzio, R.- S. Huang, J. Majer, S. Kumar, S. M. Girvin, and R. J. Schoelkopf, Nature **431**, 162 (2004).
[5] J. Bourassa, J. M. Gambetta, A. A. Abdumalikov, Jr., O. Astafiev, Y. Nakamura, and A. Blais, Phys. Rev. A **80**, 032109 (2009).
[6] T. Niemczyk, F. Deppe, H. Huebl, E. Menzel, F. Hocke, M. J. Schwarz, J. J. García-Ripoll, D. Zueco, T. Hümmer, E. Solano, A. Marx, and R. Gross, Nature Phys. **6**, 772 (2010).
[7] P. Forn-Díaz, J. Lisenfeld, D. Marcos, J. J. García-Ripoll, E. Solano, C. J. P. M. Harmans, and J. E. Mooij, Phys. Rev. Lett. **105**, 237001 (2010).
[8] G. T. Moore, J. Math. Phys. (N.Y.) **11**, 2679 (1970).
[9] V. V. Dodonov, Phys. Scripta **82**, 038105 (2010).
[10] P. D. Nation, J. R. Johansson, M. P. Blencowe, and F. Nori, Rev. Mod. Phys. **84**, 1 (2012).
[11] S. W. Hawking, Commun. Math. Phys. **25**, 152 (1972).
[12] W. G. Unruh, Phys. Rev. Lett. **46**, 1351 (1981).
[13] C. M. Wilson, G. Johansson, A. Pourkabirian, M. Simoen, J. R. Johansson, T. Duty, F. Nori, and P. Delsing, Nature (London) **479**, 376 (2011).
[14] P. Lähteenmäki, G. S. Paraoanu, J. Hassel, and P. J. Hakonen, PNAS **110**, 4234 (2013).
[15] A. V. Dodonov, R. Lo Nardo, R. Migliore, A. Messina, and V. V. Dodonov, J. Phys. B **44**, 225502 (2011).
[16] A. V. Dodonov and V. V. Dodonov, Phys. Rev. A **85**, 015805 (2012).
[17] H. Barnum, M. A. Nielsen, and B. Schumacher, Phys. Rev. A **57**, 4153 (1998).
[18] I. Devetak, IEEE Trans. Inform. Theory **51**, 44 (2005).
[19] B. Schumacher and M. A. Nielsen, Phys. Rev. A **54**, 2629 (1996).
[20] A. A. Anappara, S. De Liberato, A. Tredicucci, C. Ciuti, G. Biasiol, L. Sorba, and F. Beltram, Phys. Rev. B **79**, 201303 (2009).
[21] G. Günter, A. A. Anappara, J. Hees, A. Sell, G. Biasiol, L. Sorba, S. De Liberato, C. Ciuti, A. Tredicucci, A. Leitenstorfer, and R. Huber, Nature **458**, 178 (2009).
[22] M. A. Sillanpää, J. I. Park, and R. W. Simmonds, Nature **449**, 438 (2007).
[23] P. Meystre and M. Sargent III, *Elements of quantum optics* (4th Ed.) (Springer–Verlag, Berlin, 2007).
[24] B. Schumacher, Phys. Rev. A **54**, 2614 (1996).
[25] G. Benenti, S. Siccardi, and G. Strini, Phys. Rev. A **88**, 033814 (2013).
[26] Y. M. Wang, D. Ballester, G. Romero, V. Scarani, and E. Solano, Phys. Scr. **T147**. 014013 (2012).
[27] G. Benenti, S. Siccardi, and G. Strini, Eur. Phys. J. D **68**, 139 (2014).
[28] G. Benenti, A. D'Arrigo, and G. Falci, Phys. Rev. Lett. **103**, 020502 (2009).
[29] A. D'Arrigo, G. Benenti, and G. Falci, Eur. Phys. J. D **66**, 147 (2012).
[30] For a recent review, see F. Caruso, V. Giovannetti, C. Lupo, and S. Mancini, arXiv:1207.5435.
[31] T. Caneva, M. Murphy, T. Calarco, R. Fazio, S. Montangero, V. Giovannetti, and G. E. Santoro, Phys. Rev. Lett. **103**, 240501 (2009).
[32] K. Bergmann, H. Theuer, and B. W. Shore, Rev. Mod. Phys. **70**, 1003 (1998).
[33] A. W. Rodriguez, F. Capasso, and S. G. Johnson, Nature Photonics **5**, 211 (2011).

SUPPLEMENTARY MATERIAL

The quantum channel $\mathcal{E}$ introduced in the main text, mapping the input state ρ into the output state ρ', namely $\rho' = \mathcal{E}(\rho)$, can be conveniently described in the Fano representation (also known as the Bloch representation) [1–5]. In the RWA regime, the quantum protocol described by $\mathcal{E}$, transfers, up to a trivial unitary transformation, the state ρ from Q_1 to the cavity C, and finally from C to Q_2, leaving Q_1 and C in their ground state. More precisely, if $\mathbf{r}' = (x', y', z')$ are the Bloch ball coordinates of the final state ρ' of Q_2 and $\mathbf{r} = (x, y, z)$ the coordinates of the input state ρ of Q_1, then $x' = -x$, $y' = -y$, and $z' = z$. The state ρ can therefore be recovered from ρ' after a rotation of angle π about the z-axis of its Bloch ball. Deviations from the ideal quantum protocol appear when effects beyond the RWA cannot be neglected. In the Fano form we write $\rho = \frac{1}{2}\left(I^{(1)} + \mathbf{r}\cdot\sigma^{(1)}\right)$ and $\rho' = \frac{1}{2}\left(I^{(2)} + \mathbf{r}'\cdot\sigma^{(2)}\right)$, with $I^{(k)}$ identity operator for qubit k. Due to the linearity of quantum mechanics the Bloch vectors $\mathbf{r}$ and $\mathbf{r}'$ are connected through an affine map $\mathcal{M}$ as follows:

$$\left[\begin{array}{c}\mathbf{r}'\\ \hline 1\end{array}\right] = \mathcal{M}\left[\begin{array}{c}\mathbf{r}\\ \hline 1\end{array}\right] = \left[\begin{array}{c|c}\mathbf{M} & \mathbf{a}\\ \hline \mathbf{0}^T & 1\end{array}\right]\left[\begin{array}{c}\mathbf{r}\\ \hline 1\end{array}\right], \qquad (6)$$

where $\mathbf{M}$ is a 3×3 real matrix, $\mathbf{r}$, $\mathbf{r}'$ and $\mathbf{a}$ real column vectors of dimension 3 and $\mathbf{0}$ the null vector of the same dimension. The Fano representation of quantum operations is physically transparent since the Bloch vectors directly provide the expectation values of polarization measurements. While in general an affine map for a qubit depends on twelve parameter [6], we found from the numerical simulation of the above described quantum protocol the following structure of $\mathbf{M}$ and $\mathbf{a}$:

$$\mathbf{M} = \begin{pmatrix} m_{xx} & m_{xy} & 0\\ m_{yx} & m_{yy} & 0\\ 0 & 0 & m_{zz}\end{pmatrix}, \qquad \mathbf{a} = \begin{pmatrix} 0\\ 0\\ a_z\end{pmatrix}. \qquad (7)$$

The dependence of the six non-zero parameters, $m_{xx}, m_{xy}, m_{yx}, m_{yy}, m_{zz}$, and a_z, is shown in Fig. 5 as a function of the parameter g. Note that in the RWA limit ($g \ll 1$) we have $m_{xx} = m_{yy} = -1$, $m_{zz} = 1$, and $m_{xy} = m_{yx} = a_z = 0$, as expected for the ideal quantum state transfer protocol. On the other hand, for $g \gtrsim 0.1$ significant deviations from the ideal protocol are observed. It is interesting to remark that the positions of peaks and valleys matches those found in Fig. 2 of the

main text for the coherent information (note that here values of g up to $g = 1$ are considered). Quantum channel $\mathcal{E}$ has an interesting and non trivial structure, since it is nonunital ($\mathcal{E}(I) \neq I$ since $a_z \neq 0$) and matrix M is not symmetric ($m_{xy} \neq m_{yx}$).

The geometrical meaning of the quantum channel $\mathcal{E}$ can be understood from the decomposition of map (6)-(7) into a sequence of elementary affine maps. We first write $\mathcal{M} = \mathcal{M}_1\mathcal{M}'$, where

$$\mathcal{M}_1 = \begin{bmatrix} \cos\theta & 0 & 0 & 0 \\ 0 & \cos\theta & 0 & 0 \\ 0 & 0 & \cos^2\theta & \pm\sin^2\theta \\ 0 & 0 & 0 & 1 \end{bmatrix}, \qquad (8)$$

represents a displacements of the Bloch sphere along the z-axis [7]. Note that we have $\sin^2\theta = a_z$ or $\sin^2\theta = -a_z$ depending on the sign of a_z. In the first case the displacement of the center of the Bloch sphere is along the positive direction of the z-axis and can be seen as representative of zero temperature dissipation (amplidude damping channel [6]), in the latter case the displacement is along the negative z-direction and can be seen as thermal excitation. The affine map $\mathcal{M}'$ represents a unital quantum channel. It reads as follows:

$$\mathcal{M}' = \left[\begin{array}{c|c} \mathbf{M'} & \mathbf{0} \\ \hline \mathbf{0}^T & 1 \end{array}\right] = \begin{bmatrix} m'_{xx} & m'_{xy} & 0 & 0 \\ m'_{yx} & m'_{yy} & 0 & 0 \\ 0 & 0 & m'_{zz} & 0 \\ 0 & 0 & 0 & 1 \end{bmatrix}, \qquad (9)$$

with $m'_{ij} = (\cos\theta)m_{ij}$ for $i, j = x, y$ and $m'_{zz} = (\cos^2\theta)m_{zz}$.

Matrix $\mathbf{M'}$ can be written using the singular value decomposition as $\mathbf{M'} = \mathbf{O_1 D O_2^T}$, with $\mathbf{O_1}$ and $\mathbf{O_2}$ rotation matrices and $\mathbf{D}$ diagonal scaling matrix. Since $\mathbf{S} \equiv \mathbf{M'M'^T} = \mathbf{O_1 D^2 O_1^T}$, the diagonal entries of of $\mathbf{D}$ (known as the singular values) are the square roots of the eigenvalues of the symmetric matrix $\mathbf{S}$. We can therefore write the affine map $\mathcal{M}'$ as composition of three elementary maps, $\mathcal{M}' = \mathcal{M}_2\mathcal{M}_3\mathcal{M}_4$, with $\mathcal{M}_2$ and $\mathcal{M}_4$ rotations of the Bloch sphere about the z axis and $\mathcal{M}_3$ deformation of the Bloch sphere into an ellipsoid centred at the origin of the Bloch sphere and whose axes are directed along x, y and z. The lengths of the semi-axes of the ellipsoid are the singular values of $\mathbf{M'}$.

To summarize, the overall quantum channel $\mathcal{E}$ is obtained by the composition of a rotation of the Bloch sphere (affine map $\mathcal{M}_4$), a deformation of the Bloch sphere ($\mathcal{M}_3$), another rotation ($\mathcal{M}_2$), and a displacement of the Bloch sphere ($\mathcal{M}_1$). We need three real parameters to determine $\mathcal{M}_3$, and one parameter for each of the other transformations. Overall we have six real parameters, as also clear from Eq. (7).

Finally, we point out that a set of Kraus operators for map $\mathcal{E}$ can be easily obtained by composing the Kraus representations for the elementary transformations $\mathcal{M}_i$, $(i = 1, ..., 4)$, for which Kraus operators are well known [6].

[1] U. Fano, Rev. Mod. Phys. **29**, 74 (1957); *ibid.* **55**, 855 (1983).

[2] F. T. Hioe and J. H. Eberly, Phys. Rev. Lett. **47**, 838 (1981).

[3] J. Schlienz and G. Mahler, Phys. Rev. A **52**, 4396 (1995).

[4] G. Benenti and G. Strini, Phys. Rev. A **80**, 022318 (2009).

[5] G. Benenti and G. Strini, J. Phys. B: At. Mol. Opt. Phys. **43**, 215508 (2010).

[6] G. Benenti, G. Casati, and G. Strini, *Principles of Quantum Computation and Information*, Vol. I: Basic concepts (World Scientific, Singapore, 2004); Vol. II: Basic tools and special topics (World Scientific, Singapore, 2007).

[7] G. Benenti, S. Felloni, and G. Strini, Eur. Phys. J. D **38**, 389 (2006).

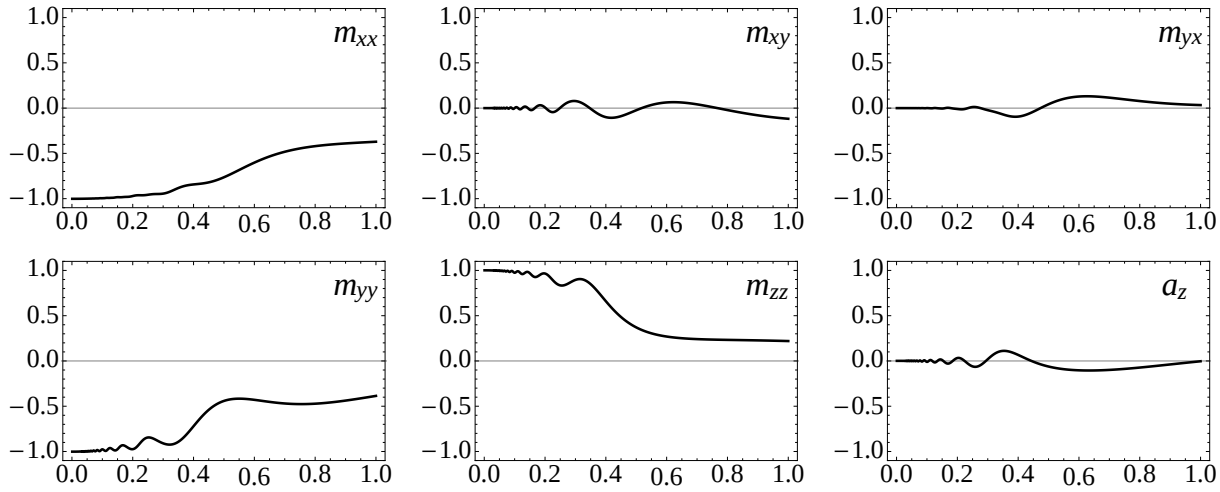

FIG. 5. Non-zero parameters of the Fano representation of the quantum channel $\mathcal{E}$, as a function of the coupling strength g, for $T_1 = T_2 = \pi/2g$, $T_c = 0$, and sudden switch on/off of the couplings.